

Design and performance of a novel multi-function debris flow mitigation system in Wenjia Gully, Sichuan

Abstract The post-earthquake debris flows in the Wenjia Gully led to the exposure of the shortcomings in the design of the original conventional debris flow mitigation system. A predicament for the Wenjia mitigation system is a large amount of loose material (est. $50 \times 10^6 \text{ m}^3$) that has been deposited in the gully by the co-seismic landslide, providing abundant source material for debris flows under saturation. A novel design solution for the replacement mitigation system was proposed and constructed, and has exhibited excellent performance and resilience in subsequent debris flows. The design was governed by the three-phase philosophy of controlling water, sediment, and erosion. An Early Warning System (EWS) for debris flow that uses real-time field data was developed; it issues alerts based on the probabilistic and empirical correlations between rainfall and debris flows. This two-fold solution reduces energy of the debris flow by combining different mitigation measures while minimizing the impact through event forecasting and rapid public information sharing. Declines in the number and size of debris flows in the gully, with increased corresponding rainfall thresholds and mean rainfall intensity-duration (*I-D*) thresholds, indicate the high efficacy of the new mitigation system and a lowered debris flow susceptibility. This paper reports the design of the mitigation system and analyzes the characteristics of rainfall and debris flow events that occurred before and after implementation of the system; it evaluates the effectiveness of one of the most advanced debris flow mitigation systems in China.

Keywords Wenjia mitigation system · Debris flow · Early Warning System · Wenchuan Earthquake · Co-seismic landslide

Introduction

Wenjia Gully has become one of the most studied geohazard sites in China since the 2008 Wenchuan Earthquake. The co-seismic landslide and subsequent debris flows represent a classic post-earthquake instability process. It poses challenges to mitigation measures, as a huge amount of poorly sorted landslide deposits are being transformed into source material for rainfall-induced debris flow. The saturation of the poorly sorted sediment induces sudden downward surges under gravitational forces (Iverson 1997). In the case of the Wenjia Gully, the loose sediments deposited by the co-seismic landslide are mobilized by the intense surface run-off due to excessive rainfall (Xu et al. 2012; Zhou et al. 2014).

The gully is located on the left bank of the Mianyuan River in the Qingping area near Mianzu County in Sichuan (Fig. 1b). It is situated less than 4 km SE of the Yingxiu-Beichuan thrust fault and 80 km NE of the epicenter of the 2008 Wenchuan Earthquake (M_S 8.0). The depth of the gully was 30–50 m with a length of 3 km (highest elev. 2402 m) and an average slope gradient of 45° before the earthquake; it had extensive vegetative coverage with an area exceeding 80% of the basin (Wang et al. 2014). The gully is situated on the Guanwushan Group (Upper Devonian Period) and

Qingping Group (Cambrian Period) in sequence. The Guanwushan Group (th 182 m) consists of mainly carboniferous limestone, and the Qingping Group (th 488 m) comprises mainly sandstone and siltstone. Loose Quaternary deposits were found in the form of terraces and alluvial fans in the gully (Xu 2010).

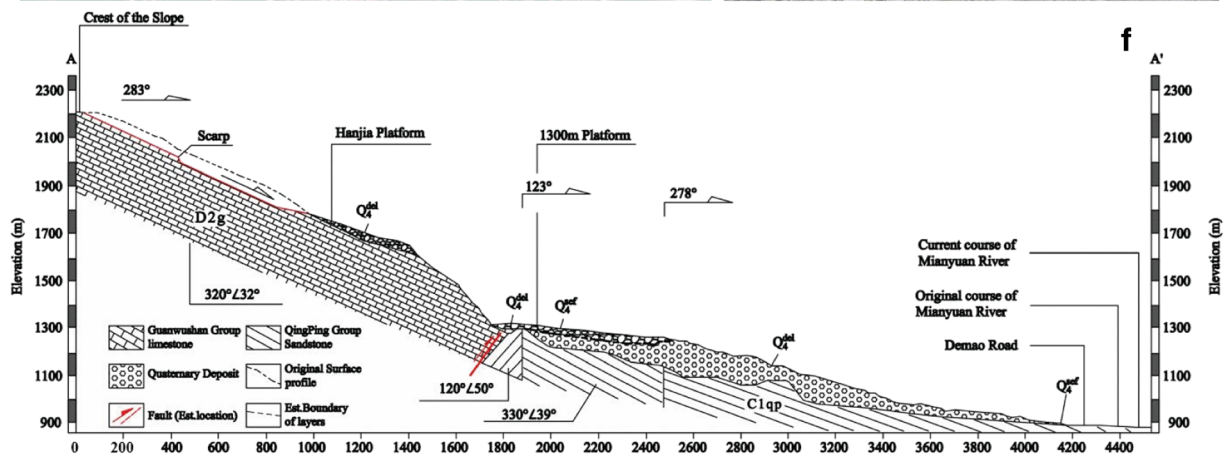
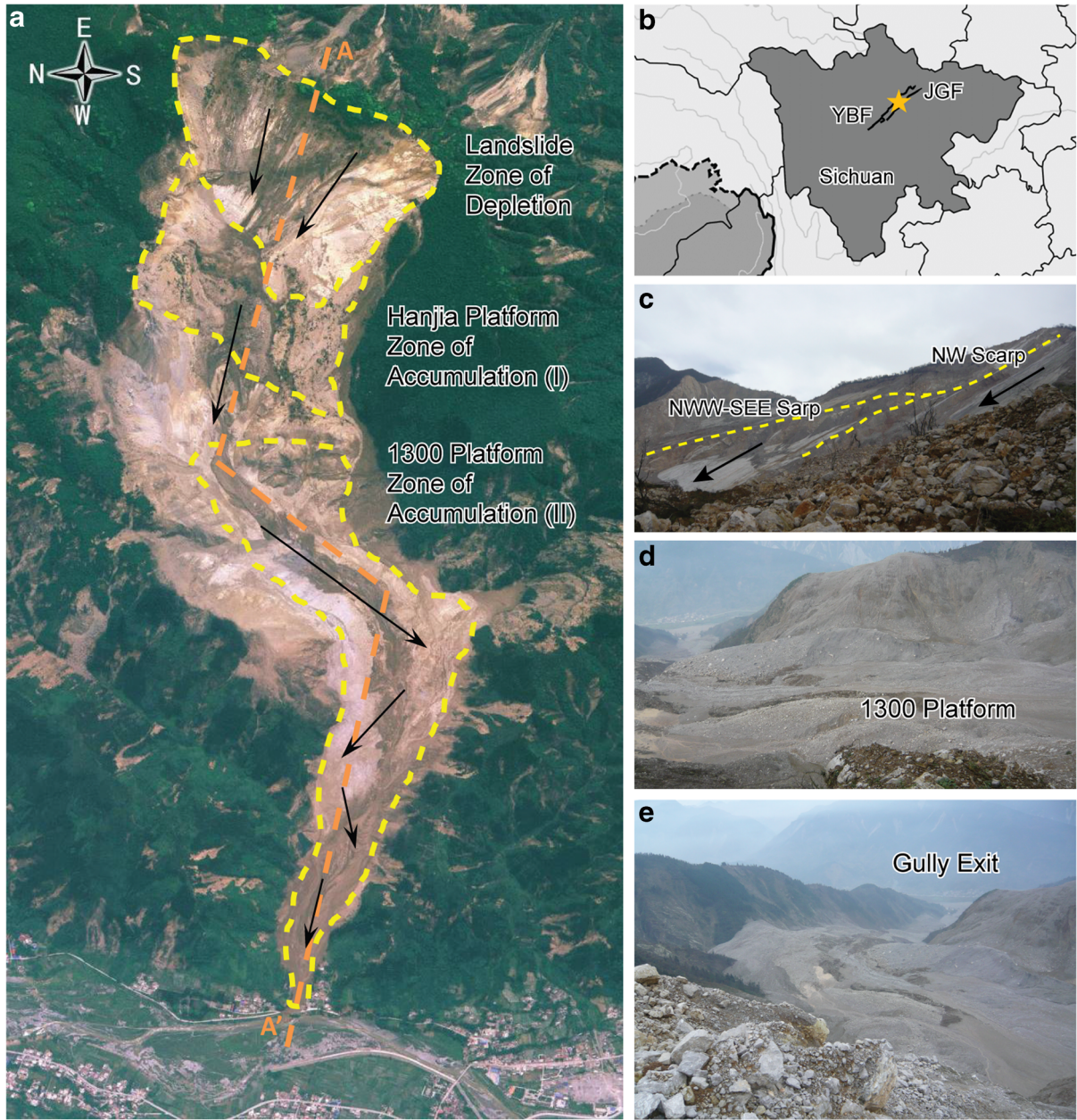
The study area is in a subtropical monsoon climate zone with rainfall concentrated in the monsoon season that spans from June to September (typically 60% of the annual rainfall). The average annual rainfall is 1086.4 mm with an average temperature of 14.4°C . Prior to the Wenchuan Earthquake, the highest recorded annual rainfall is 1421.4 mm in 1963 and the lowest is 699.3 mm in 1965; the highest daily cumulative rainfall was 500 mm on August 15, 1995, and the highest peak rainfall intensity was 49.8 mm/h on August 11, 1995. No record of debris flows in the Wenjia Gully was found before the earthquake, although at least 18 debris flows have occurred in the adjacent gullies in the past two decades.

The ground shaking caused a deep-seated co-seismic landslide in the gully that initiated at an elevation of 1780–2340 m. Two main scarps were observed orientating WNW-SEE and NW (Fig. 1c); it was postulated that the displaced materials originated from the two adjacent limestone rock blocks. The total volume of the rock blocks was $27.5 \times 10^6 \text{ m}^3$, of which nearly 70% remained on the Hanjia Platform, while the rest entered the 1300 m Platform (a platform at the elevation of 1300 m) as shown in Fig. 1d. The landslide transformed into a rock avalanche and entrained a large amount of shallow sand-gravel materials during its movement (Xu et al. 2009; Xu 2010). The estimated volume of loose deposits in the 1300 m Platform and the Zone of Accumulation II was $30 \times 10^6 \text{ m}^3$ (Fig. 1d, e). Based on the characteristics of the deposits, a hypothetical flow trajectory for the landslide was proposed and delineated as shown in Fig. 1a.

After the Wenchuan Earthquake, many co-seismic landslides were followed by debris flows and sediment flux in the affected catchments with catastrophic consequences due to underestimation on the potential for such events (Huang and Fan 2013). Debris flow mitigation measures were installed after the debris flow in September 2008 but failed disastrously in 2010 under the continuous impacts of the events. A new mitigation system was designed and constructed in 2011, which, to date, has exhibited excellent performance in preventing debris flows from reaching the downstream community, while maintaining a high level of resilience to debris flows itself. In this paper, the large-scale debris flows that have occurred after the earthquake are discussed, and the implementation of the mitigation system is described.

Pre-mitigation debris flows

In 2008, the monthly precipitation in the Qingping area in June, July, August, and September were 113, 167.5, 170, and 350 mm, respectively. Several small-scale debris flows occurred in the Wenjia Gully during the rainstorms on June 18–21 and July 24–25. The first major debris flow occurred on September 24, during which the daily rainfall was 88 mm with a peak 10-min rainfall of



◀ **Fig. 1** The landslide/rock avalanche induced by the 2008 Wenchuan Earthquake. **a** Post-earthquake image of the gully, with the possible landslide moving trajectory (Image: May 23, 2008). **b** Location of the study area. *YBF* Yingxiu-Beichuan Fault, *JGF* Jianguyou-Guanxian Fault. **c** The scarps of the co-seismic landslide. **d** Image of the 1300 m platform. **e** Image of the Zone of Accumulation II. **f** The geological profile of cross section A-A'

11.5 mm. The intense surface run-off mobilized the loose deposits in the Zone of Accumulation I and II (Fig. 2a), and resulted in channelized erosion and deep incisions (approx. 20 m) in the gully (Fig. 2b, c). The volume of the debris flow was estimated as $0.5 \times 10^6 \text{ m}^3$, which is less than 1% of the loose deposit in the gully (Xu et al. 2009), but it destroyed the infrastructure near the outlet of the gully and part of the Qingping area. The deposit from the debris flow formed a dam and resulted in water impoundment in the Mianyuan River.

Mitigation measures were proposed after the debris flows in 2008, which include a debris basin and a drainage channel with two check dams located at the lower end of the Hanjia Platform and near the exit of the gully. The design of the mitigation measure was modified in the following year by adding 19 more check dams between 1243 and 1095 m (elev.), with lengths of 20.5–84 m and an average height of 4.5 m. A diversion dike was constructed in the Zone of Accumulation II with six sectional barriers between 1095 and 1075 m (elev.). Retaining structures were constructed on the hillsides with 35 sectional barriers between 1075 and 985 m (elev.). A check dam was built near the outlet of the gully (elev. 940 m) spanning 215 m between both sides of the gully, for which the height was 8 m with a large debris basin. A main drainage channel

with a length of 255 m was designed containing 12 sectional barriers and retaining structures on both sides. The mitigation measures were completed in early July 2010 but were severely damaged by the end of the month; nine check dams were destroyed and the volume of deposit in the debris basins reached the maximum design level.

The debris flow that occurred on August 13, 2010, has been well studied and presented in the literature (Xu 2010; Ni et al. 2012; Tang et al. 2012; Xu et al. 2012; Yu et al. 2013, 2014; Zhou et al. 2014). A heavy rainstorm was reported with rainfall being concentrated between 14:00 on August 12 and 01:00 on August 13 (daily cumulative rainfall $R_d = 220 \text{ mm}$; peak rainfall intensity $I_{max} = 70 \text{ mm/h}$). According to eyewitnesses, the debris flow lasted for about 2 h from 01:00 to 03:00 on August 13, which coincided with the duration of the rainfall in the gully. The heavy rainfall generated intense surface run-off, which saturated the loose deposit and produced a large erosion channel with a depth of 60 m and a slope gradient of 60° (Fig. 3a, b). The debris flow was intercepted by the check dam at the outlet of the gully until its failure (Fig. 3c). The estimated debris volume exceeded $4.5 \times 10^6 \text{ m}^3$, and it covered a total area of 635,000 m^2 in the Qingping area (Xu et al. 2012). The debris flow deposit has an average thickness of 7 m (max. >15 m) (Fig. 3f). The deposits blocked the Mianyuan River (Fig. 3g) along with compounding debris flows in the area, including a large-scale event in the Zoumaling Gully located 4 km upstream of Wenjia Gully. The Qingping area was severely damaged and partially buried by the debris flows, which caused 7 casualties, 39 injured, and 497 houses buried (Yu et al. 2013). Another debris flow developed in the gully on August 19 due to heavy rainfall, which

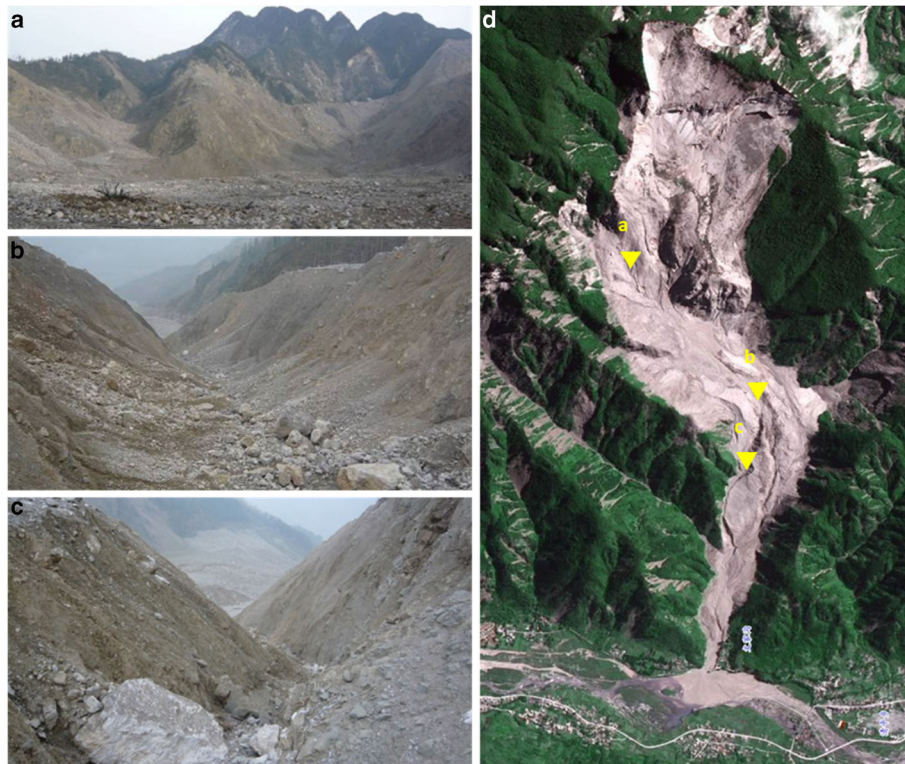


Fig. 2 Images of the Wenjia Gully after the debris flow on September 24, 2008. **a** Loose deposit near the toe of the Hanjia Platform. **b** Channelized erosion in the Zone of Accumulation II. **c** Deep incision due to surface run-off. **d** Post-debris flow image (Image: Oct 13, 2008)



Fig. 3 The devastating debris flow occurred on August 13, 2010. **a** Deep incision due to channelized erosion on the 1300 m Platform. **b** Widened debris flow channel near the outlet of the gully. **c** Failure of the last check dam (after Tang et al. 2012). **d** A buried house in Qingping Village (August 13, 2010). **e** Increase in the thickness of the deposit after a subsequent debris flow (August 19, 2010). **f** Submerged area near the outlet of the gully. **g** Aerial image of the debris flow with approximated locations of the images presented herein

interrupted the rapid-response construction of mitigation measures and deposited an additional $17.6 \times 10^4 \text{ m}^3$ of sediment (Fig. 3d, e).

Design of the mitigation system

The design of the conventional mitigation system which followed the standard design code (Ministry of Land and Resources of China 2006) underestimated the discharge and volume of the debris flows due to inadequate consideration of the characteristics of the source materials and rainfall thresholds. Without considering the post-earthquake scenarios, the estimated volume of debris flow in the Wenjia Gully was, on average, 45% less than that observed between 2008 and 2010; the observed volume of the debris flow on August 13, 2010, was 12 times greater than the estimate based on the design code.

A design solution for the debris flow mitigation system was proposed by the State Key Laboratory of Geohazard Prevention and Geoenvironment Protection (SKLGP) (Xu 2010; Xu et al. 2012); it integrates three key elements, including the water-sediment segregation (water control), source material stabilization (sediment control), and channelized erosion prevention (erosion control). As a debris flow is a mixture of loose solids and fluid, the aim of the mitigation system is to minimize surface run-off by separating the fluid and solid components of the debris flow. The stabilization of the loose deposit in the Zone of Accumulation II reduces the source material, which in turn, decreases the size of the debris flow. The development of an erosion channel which was

typical after debris flows in the gully indicated a high level of energy from surface run-off. The channelized erosion can easily damage a rigid drainage system and mobilize additional loose deposits. A novel drainage channel was designed by allowing a certain degree of flexibility in the system, which has proven to be effective in preventing channelized erosion caused by debris flows. Field instruments were deployed in the gully as part of the development of the Early Warning System.

The debris flow mitigation system has a designed seismic resistance of VII on the Mercalli Intensity scale and was completed in May 2011 (Fig. 4). Reflecting the proposed design, the system has three key sub-systems: (1) a combined sediment basin and debris flow breaker with a drainage tunnel in the upstream section of the gully, (2) a flexible drainage channel in the mid-region of the gully to “guide” the movement of debris flows, and (3) five check dams in the upstream and downstream sections of the gully. A service road was excavated parallel to the flexible drainage channel to allow access by equipment for periodic emptying and maintenance of the debris basins. Part of the Zone of Accumulation II was excavated for the construction of the drainage channel.

Upstream

The mitigation measures in the upstream section of the gully are shown in Fig. 5. The primary source materials for debris flows in the upstream region are from the loose deposits in Branches #3, #4, and #5. The landslide deposits in these branches are poorly sorted with an

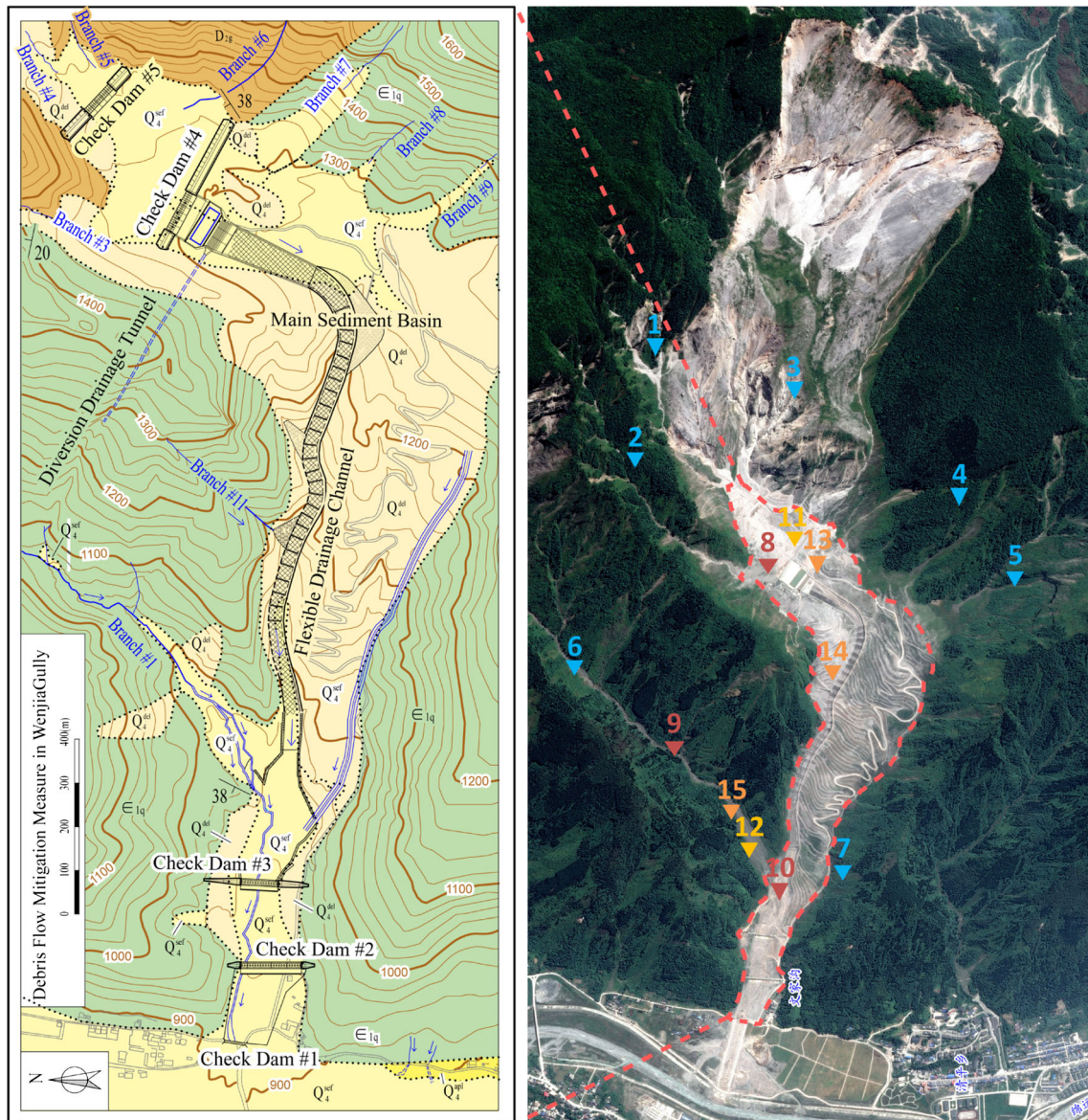


Fig. 4 The debris flow mitigation system in the Wenjia Gully. Check Dams #4 and #5 are located upstream between the Hanjia Platform and 1300 m Platform. The midstream section consists of a flexible drainage channel. Three check dams were constructed in the downstream of the gully. A large number and variety of sensors were installed in the gully and/or its catchment, including the rain gauges (1–7), thickness gauges (8–10), piezometers (11–12), and video cameras (13–15)

average D_{90} of 1 m; the thickness is 60–80 m and is overlain by 10 m of subsequent debris flow deposit. The construction of Check Dam #5 was intended to intercept the loose deposits mobilized from Branches #4 and #5 (Fig. 5a), while reducing the slope gradient below the Hanjia Platform. Check Dam #4 is located downstream of Check Dam #5; its main functions are (1) to provide additional capacity in the debris basin and (2) to accommodate the debris-flow breaker and re-route the water of the debris flow into the drainage tunnel. A reflection wall was constructed and connected to Check Dam #4 to prevent the potential impact of the deposits from Branch #3. The design capacities of the debris basins for Check Dams #4 and #5 are 82.6×10^3 and 57.7×10^3 m³, respectively.

A sediment basin was constructed downstream of Check Dam #4 integrated with a debris flow breaker system and forms a water-

sediment segregation system (Fig. 5b). The depth of the sediment basin is 4 m with the areas of the top and bottom of 40×106 and 27×85 m², respectively. The breaker system consists of four arrays of steel fins (Fig. 5c) aligned perpendicular to the dominant flow direction. The water-sediment segregation system is critical to the entire mitigation system. As the catchment area is over 4 km², the upstream region of the gully is susceptible to flood and hyperconcentrated flow that may transform into debris flow. In the event of overtopping of Check Dams #4 and #5, the sediment basin slows down the debris flow surge and reduces the dynamic impact by permitting rapid settlement of larger boulders and rocks. The breaker system enables rapid drainage of surface runoff through the drainage tunnel, which in turn, prevents erosion and mobilization of the loose particles at the 1300 m Platform and

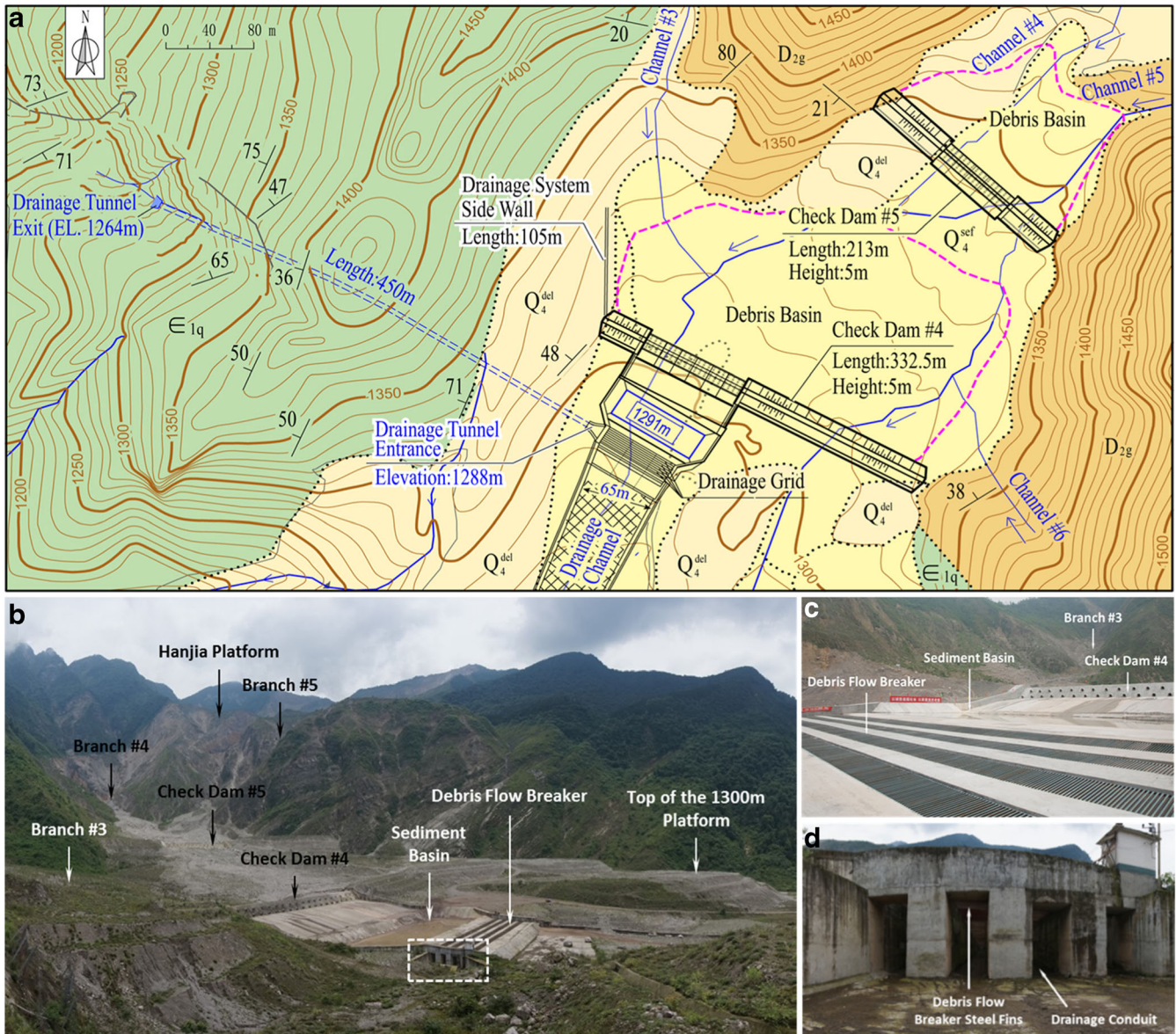


Fig. 5 The mitigation measures in the upstream section of the Wenjia Gully. **a** A plan view of the mitigation structures. **b** An overview of the mitigation structures. **c** The water-sediment segregation system formed by a sediment basin and a breaker system. **d** The drainage conduits underneath the steel fins of the debris flow breaker

in the rest of the Zone of Accumulation II. The sediment basin optimizes the efficiency of the breaker system by cushioning the impact of surge waves and improves the longevity of the breaker. Fluid and small-scale sediment removed from the bulk of the debris flow are drained through the drainage tunnel (Fig. 5c) and discharged to Branch #1 (Fig. 5d). The tunnel has a design discharge capacity of $106.5 \text{ m}^3/\text{s}$ and a length of 450 m at a gradient of 0.05 with a width and height of 4.5 and 3.5 m, respectively.

The core of the design is to stabilize the loose deposits at the 1300 m Platform by re-routing the fluid component of the debris flow. Check Dams #4 and #5 are considered sufficient to intercept most of the mobilized sediments from Branch #4 and #5, as the amount in these tributary gully branches is comparatively small. Following the same line of reasoning, debris flows in Branch #1 poses a smaller impact even under intense surface run-off from rainfall and the fluid exiting from the drainage tunnel.

Midstream

The mitigation structure in the mid-region of the gully is a stepped flexible drainage channel extending from the debris flow breaker system to the outlet of the gully (Fig. 6a). The channel has a total length of 1290 m containing 25 steps at an average interval of 27 m with widths ranging from 45 m (upstream end) to 30 m (downstream end); it aims to reduce the volume of debris flow by minimizing erosion using gabion basket modules (Fig. 6b). The gabion modules buttress riprap that consists of angular and resistant rocks, which deforms under the impact of a debris flow without significant reduction of its efficiency (Costa and Wiczorek 1987). The stepped chute promotes kinematic energy dissipation, which drastically decreases the discharge rate of the debris flow, and in turn, the impact to the midstream and downstream of the gully by minimizing the energy (i.e. discharge control) and reducing the volume of the debris flow (i.e. erosion control).

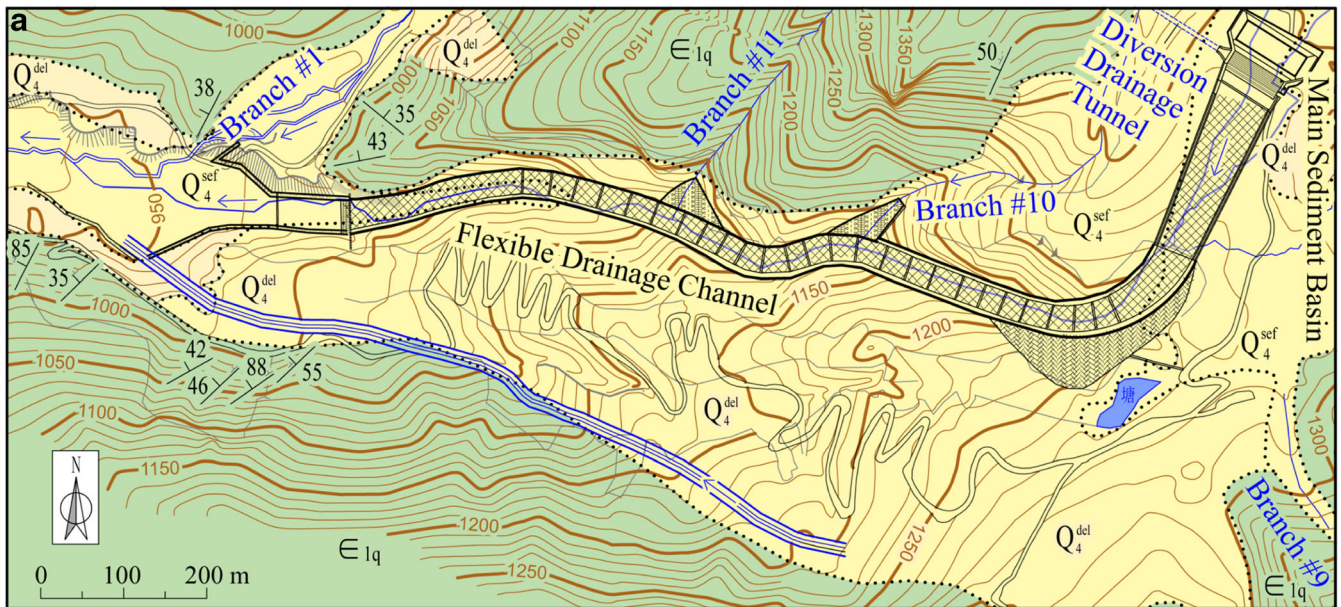


Fig. 6 The mitigation measures in the midstream section of the Wenjia Gully. **a** A plan view of the mitigation structures. **b** An overview of the flexible drainage channel. **c** A close view on the stepped channel on the 1300 m platform. **d** Terraced loose deposits on the south of the channel with ground seeding and LEBs for stabilization

The upstream end of the channel is connected to the water-sediment segregation system, and a pile system (23 piles) was installed at the downstream end (Fig. 6b). Retaining structures were constructed on both sides of the channel (Fig. 6b, c). A service road was excavated on the hillslope located to the south of the channel, where a large amount of sediment was deposited due to construction of the channel.

The local topography was altered into terraced landscape, and additional erosion control methods were applied, including ground seeding, mulching, and small-scale log erosion barriers (LEBs), to stabilize the loose deposits. The LEBs are installed on the road embankments and ground seeding applied in this area (Fig. 6d). The LEBs are made of bamboos and held in place by steel poles, which serve as mechanical

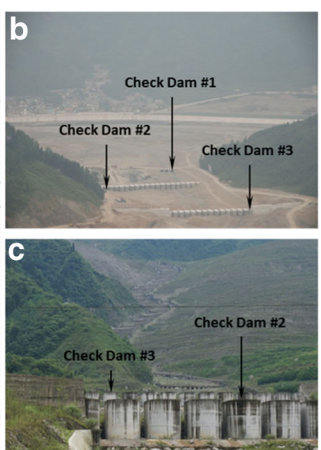
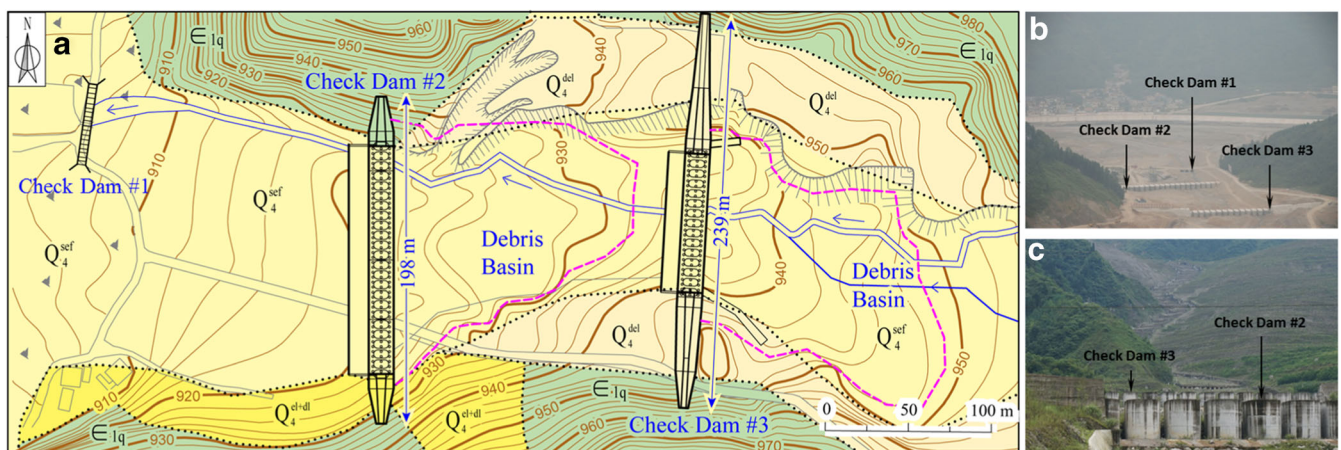


Fig. 7 The mitigation measures in the downstream section of the Wenjia Gully. **a** A plan view of Check Dam #1 (for pedestrian assess), #2, and #3 and the debris basins. **b** An overview of the check dams on near the exit of the gully. **c** A close view on the concrete fins of Check Dam #2 (image taken from Check Dam #1)

retaining racks and reduce rill erosion while promoting seepage (deWolfe et al. 2008). One smaller drainage channel was constructed parallel to the flexible drainage channel to prevent erosion by surface

run-off of the treated hillslope. Three piezometers were installed along the flexible channel to provide real-time monitoring on the groundwater table which may pose risk to the stability of the structure.

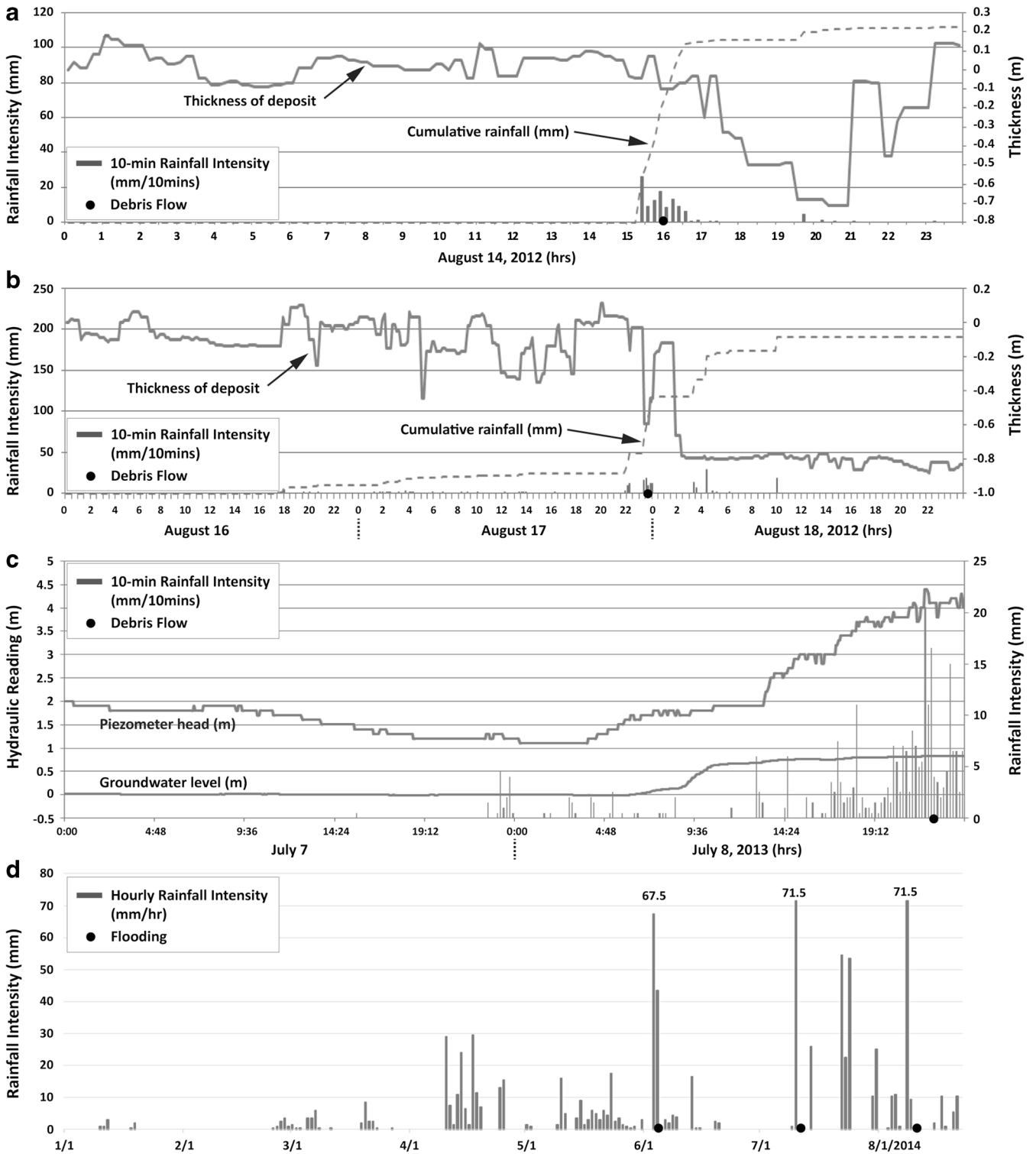


Fig. 8 Field data of the post-mitigation debris flows from 2012 to 2014. The rainfall data were gathered near Branch #4 and #1, and thickness readings were recorded near Check Dam #3. **a** Evident temporal and spatial correlations between rainfall and deposit thickness as demonstrated in the debris flow on August 24, 2012. **b** Rapid decrease in the deposit thickness in Branch #1 was captured indicating the initiation of the debris flow on August 17, 2012. **c** Field data of the debris flow on July 7–11, 2013. **d** Relation between floods and peak rainfall intensity in 2014

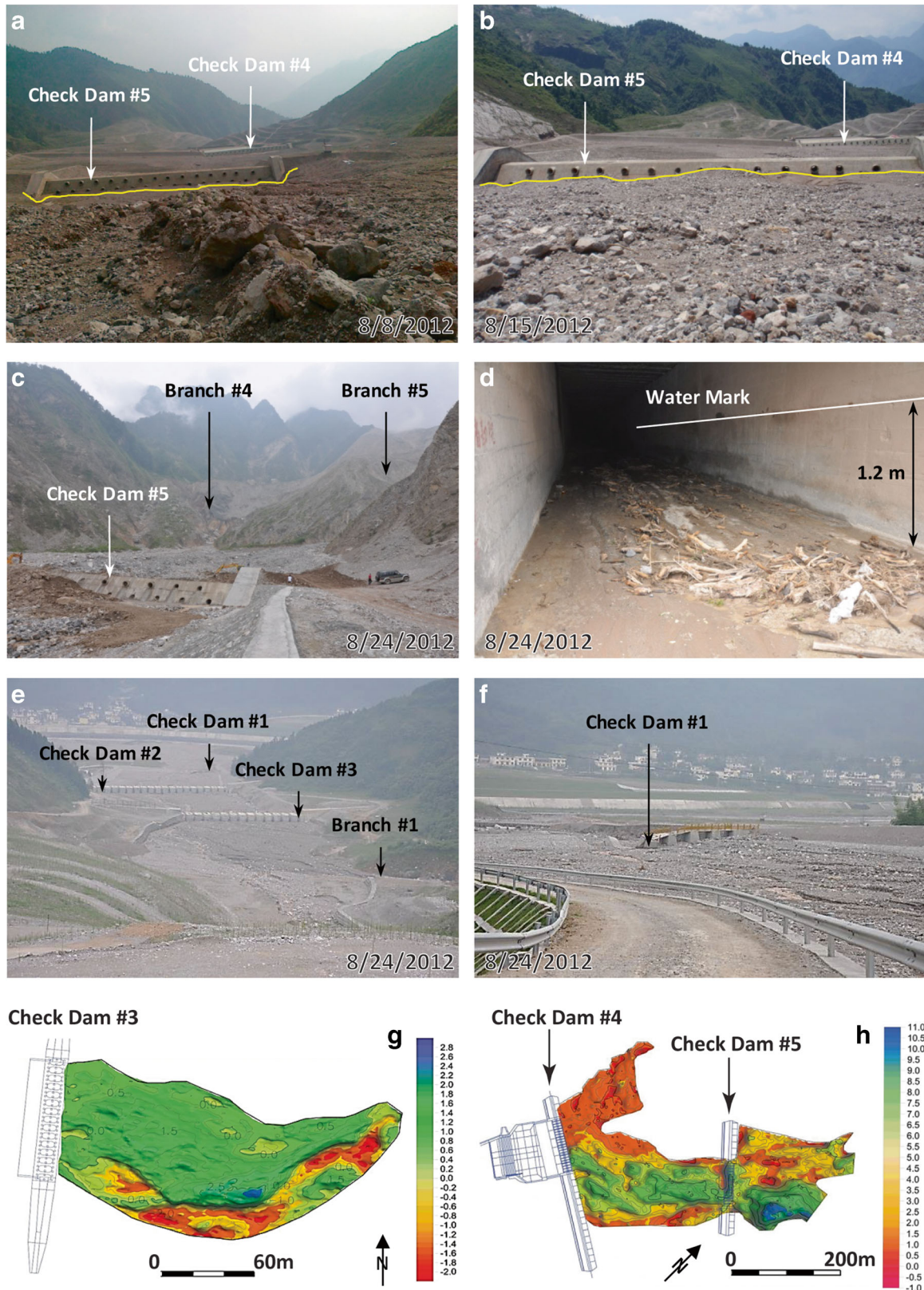


Fig. 9 The pre-/post-debris flow images in the monsoon season of 2012 and the elevation difference in the debris basin between August 2012 and July 2013. **a** Surface profile of the deposit in the basins. **b** Surface profile of the deposit after the debris flow on August 14 showing change in the thickness of the basin. **c** Overtopping of Check Dam #5 due to the debris flow on August 17. **d** Water level in the drainage tunnel. **e** Deposit in the debris basins of Check Dam #2 and #3 after the debris flow on August 17. **f** Damaged Dam #1 due to the erosion by the debris flow initiated in Branch #1. **g** Debris basin variations in Check Dam #3 showing evident scouring in the deposit on the south side of the basin. **h** Debris basin variations in Check Dam #4 and #5 showing surface erosion caused by loose deposits mainly from Branch #3

Table 1 Major rainfall and debris flow events in the Wenjia Gully before and after the Wenchuan Earthquake as well as the completion of the debris flow mitigation system

Date	I_m (mm/hr)	I (mm/hr)	R_d (mm)	R_t (mm)	RI (cm^2/hr)	RTI (cm^2/hr)	D (hr)	Debris Flow	V (10^4 m^3)	A (10^4 m^2)
7/27/1992	35.2		232.3	464.6*	57.363	122.69		○		
7/15/1993	31.7		233.0	466.0*	25.025	69.615		○		
9/09/1994	25.0		56.00	112.0*	36.570	40.015		○		
8/15/1995	49.8		496.5	993.0*	36.450	67.770		○		
8/26/1996	34.4		221.1	442.2*	24.752	59.378		○		
8/15/1997	20.0		110.2	220.4*	25.383	29.110		○		
9/17/1998	39.3		290.0	580.0*	81.770	163.54		○		
8/15/1999	49.8		100.8	201.6*	73.861	147.72		○		
7/29/2000	23.9		148.4	296.8*	14.000	28.000		○		
8/19/2001	35.1		258.9	517.8*	247.26	494.51		○		
7/31/2002	20.3		104.0	208.0*	76.058	152.12		○		
8/09/2003	38.9		227.0	454.0*	22.040	44.080		○		
7/26/2004	22.8		58.30	116.6*	113.97	227.94		○		
7/19/2005	33.9		126.2	252.4*	50.198	100.40		○		
9/24/2008	30.5	7.30	44.00*	88.00	35.468	70.935	12	●	50	12
8/25/2009	28.9		43.35*	86.70	90.874	181.75		○		
7/25/2010	11.6		44.80*	89.60	21.112	42.224		●		
7/31/2010	51.7	17.9	60.20	89.50	88.303	176.61	5	●	60	
8/13/2010	70.6	17.2	137.6	227.5	13.292	26.585	7	●	310	63.5
8/19/2010	69.0	11.1	122.2	251.0	42.782	85.564	11	●	30	12
9/18/2010	29.0	22.5	26.00*	52.00	12.528	25.056	3	●	17.6	8.5
9/22/2010	24.5		40.60*	81.20	9.9470	19.894		○		
8/21/2011	13.6		38.30*	76.60	5.2088	10.418		○		
8/14/2012	73.5	47.2	138.5	138.5	21.503	43.310	3	●	3.16	1.56
8/17/2012	71.5	60.3	180.5	280.0	0.7175	2.8525	11	●	7.8	6.4
6/13/2013	30.5		70.50	142.0	5.4050	13.685		○		
6/28/2013	32.5		176.5	377.5	1.9200	2.7000		×		
7/06/2013	59.0	41.5	311.5	858.0	2.1000	8.1000	29	●	34.4	
7/25/2013	45.5		55.00	153.0	0.2625	0.7375		×		
8/06/2013	26.5		138.0	151.0	5.8125	9.0675		×		
9/01/2013	3.50		20.50	81.50	13.420	26.840		○		
9/15/2013	11.5		47.00	119.0	5.1968	10.394		○		
5/09/2014	12.0		16.00	22.50	31.123	46.272		○		
5/14/2014	12.0		17.50	67.50	97.146	160.62		○		
6/03/2014	54.0		67.50	125.5	84.318	173.19		×		
7/22/2014	45.5		54.40	130.5	7.5400	15.080		×		
8/08/2014	35.5		71.50	82.00	101.80	101.80		×		
8/20/2014	2.50		10.50	29.50	129.06	200.20		○		
9/20/2014	15.5		37.50	58.50	183.79	506.22		○		

This table includes some of the historical rainfall data from the local metrological stations. No known debris flow occurred in the Wenjia Gully before the earthquake, but rainfall has induced debris flows in the adjacent gullies. Dash lines represent the earthquake and completion of the new mitigation system

I_m and I are the peak and mean rainfall intensity, respectively; R_d and R_t are the daily cumulative and 7-day antecedent rainfall, respectively; RI is the Rainfall Index ($RI = R_d I_m$); RTI is the Rainfall Triggering Index ($RTI = R_t I_m$); D is the rainfall duration; V and A are the estimated volume and covering area of debris flow, respectively; ● pre-mitigation debris flow; ● post-mitigation debris flows; ○ no debris flow; × flood or hyperconcentrated flow

^a Assuming $R_d = 1/2R_t$, as proposed by Yu et al. (2013)

Downstream

The mitigation system in the downstream section of the channel focuses on intercepting the medium and large boulders and rock masses from Branches #1 and #2 as well as any possible far-reaching sediments that originate from the upstream (Fig. 7a).

The main structures consist of three check dams with sectional barriers and concrete fins (Fig. 7b, c). Check Dam #2 has a height of 6 m above ground level with a design width for overflow of 139 m and a maximum volume of $67.5 \times 10^3 \text{ m}^3$ for the debris basin. Check Dam #3 has a height of 5 m with a design capacity of the

design basin of $25.6 \times 10^3 \text{ m}^3$. Check Dam #1 was added after the completion of the system, with the primary purpose being pedestrian access while serving as the last barrier for debris flows. Deflection and retaining walls were built to protect and stabilize the hillsides in the downstream.

The design of the check dams was based on the debris flows induced by a peak rainfall intensity of 91.9 mm/h, which, according to the design code, yields $36.4 \times 10^4 \text{ m}^3$ of sediments (Ministry of Land and Resources of China 2006). The opening of the fins must be sufficiently small to prevent large particles of sediment from reaching the Qingping area. Since the sediment deposited near the outlet of the gully from the debris flow in August 2010 had a maximum particle size of 1.0 m, the first sectional barrier of Check Dam #3 was designed with a fin gap of 1.5 m to intercept the sediment with sizes greater than 0.8 m. Check Dam #2 has a fin gap of 1.0 m to retain the deposits with sizes greater than 0.6 m.

Early warning system (EWS)

A EWS was developed for each gully in the Qingping area (20 gullies) that experienced continuous debris flows after the earthquake; it utilizes the real-time data collected by the field instruments. The locations and types of monitoring devices in the Wenjia Gully are shown in Fig. 4. The datasets are acquired, stored, and integrated into a 3-D WebGIS-based platform that consists of a support layer, a service layer, and a client layer. The support layer transmits the monitoring dataset, the service layer integrates data and geospatial information on the publicly available map server, and the client layer provides an end-user interface for data query and visualization. The service layer provides real-time warning based on probabilistic and empirical correlations between rainfall and debris flow occurrences. The EWS issues warning signs representing different danger levels to the registered users.

A variety of rainfall-induced debris flow prediction models were tested in the design of the EWS for the Wenjia Gully (Glade et al. 2000; Guzzetti et al. 2007, 2008; Cannon et al. 2008). As the occurrence of debris flows has exhibited correlations with $I_{max} R_d$ and the antecedent rainfall, the EWS monitors and issues alerts based on the designated rainfall thresholds (Zhuang et al. 2014; Huang et al. 2015a, b). Due to limited data availability for debris flows in the Wenjia Gully, the thresholds were initially established by using the historical rainfall data, but the model and thresholds are updated annually. Detailed discussion on the EWS is presented by Huang et al. (2015a).

Performance of the mitigation system

Post-mitigation debris flows

Three heavy rainstorms occurred in the gully between May and June 2011; the first two were on May 9 and June 16, respectively. The third rainstorm was the largest and lasted from June 30 to July 4 with a peak 10-min rainfall of 10.5 mm and a cumulative precipitation of 387 mm; however, no debris flow was observed in the Wenjia Gully. Two large-scale debris flows occurred on August 14 and 17. A rainstorm swept over the study area between 15:00 and 17:10 on August 14 ($R_d = 138.5 \text{ mm}$; $I_{max} = 50 \text{ mm/h}$) (Fig. 8a). The debris flow lasted for about 2 h and mobilized the loose deposits in Branches #4 and #5. The decrease in the surface level of the deposits in the channel was captured by the thickness gauge, indicating a small-scale debris flow (Fig. 8a); it was followed by two additional ones that possibly originated from Branch #1 and

resulted in the spikes at 21:00 and 23:00 (Fig. 8a). The debris flow was largely blocked by Check Dam #5, but an erosion channel was formed in the basin of Check Dam #4. The estimated volume was over $31,500 \text{ m}^3$ covering a total area of $15,600 \text{ m}^2$.

The debris flow on August 17, 2012, was induced during a rainfall event that occurred intermittently between 01:00 on August 17 and 05:00 on August 18 (Fig. 8b). Rainfall started at 01:10 on August 17 and paused for 14 h before the subsequent rainstorm at 22:50 ($R_d = 280 \text{ mm}$; $I_{max} = 71.5 \text{ mm/h}$); it lasted for nearly 5 h and resulted in debris flows in Branches #3, #4, and #5. The increases in the levels of deposit in the upstream debris basins became more pronounced after the debris flow on August 17 (Fig. 10a, b). The loose deposits overtopped Check Dams #5 and #4 and settled on the steel fins with rapid drainage of fluid. The water mark in the drainage tunnel indicated the height of the flow which was 1.2 m at the entrance with an estimated peak flow discharge of $49.1 \text{ m}^3/\text{s}$ (Fig. 9d). The discharge in the drainage tunnel mobilized the loose deposit in Branch #1 (the exit of the tunnel). A considerable amount of sediment was deposited in the debris basins near the outlet of the gully (Fig. 9e), where the surface run-off eroded and undermined the foundation of Check Dam #1. The scouring and erosion caused differential settlement, and ultimately the failure of Check Dam #1 (Fig. 9f), but the debris flow did not cause any damage to the downstream community. The volume of the deposit was estimated as $78,000 \text{ m}^3$ covering a total area of $80,000 \text{ m}^2$, by using LiDAR scans for the debris basins between June 24 and August 24.

In 2013, rainstorms were reported in the gully on June 18–20, June 29, July 1, July 3–5, and July 7–11 ($R_d = 836.5 \text{ mm}$; $I_{max} = 71 \text{ mm/h}$). Many of the monitoring instruments were defective due to inadequate maintenance. Field data is summarized and shown in Fig. 8c, but the exact time of the occurrence of the debris flow cannot be determined. Interviews with local residents confirmed that the debris flow occurred at 22:00–23:00 on July 8. The loose deposits in Branches #4 and #5 provided the source material, with significant incision and undercutting in both branches. The debris flow reached the debris basin of Check Dam #4 and damaged the left flank of the dam. A considerable amount of water entered the drainage tunnel causing minor erosion in Branch #1, which in turn mobilized and deposited some sediments in the debris basin of Check Dam #3. The total volume of the debris flow was estimated as $344,000 \text{ m}^3$ based on the changes of the thickness of deposit in the debris basins (Fig. 9g, h).

Three small-scale hyperconcentrated flows occurred during the monsoon season on June 3, July 10, and August 8, 2014. The rainfall data were collected and are presented in Fig. 8d. Two of them are considered as floods because of the small amount of deposit material.

Post-mitigation rainfall thresholds

At least nine large-scale debris flows have occurred in the Wenjia Gully between 2008 and 2015. The associated rainfall parameters, including the peak rainfall intensity I_m , daily cumulative rainfall R_d , 7-day antecedent rainfall R_7 , Rainfall Index (RI), and Rainfall Triggering Index (RTI), are summarized in Table 1. The antecedent rainfall R_7 is defined by Jan et al. (2002, 2004). The Rainfall Index (RI) is defined as the product of $R_d I_m$ (Chen et al. 2013), and the Rainfall Triggering Index is expressed as the product of $R_7 I_m$ which can be used to establish the associated probability of debris flow occurrences in the prediction model (Jan et al. 2002; Jan and Lee

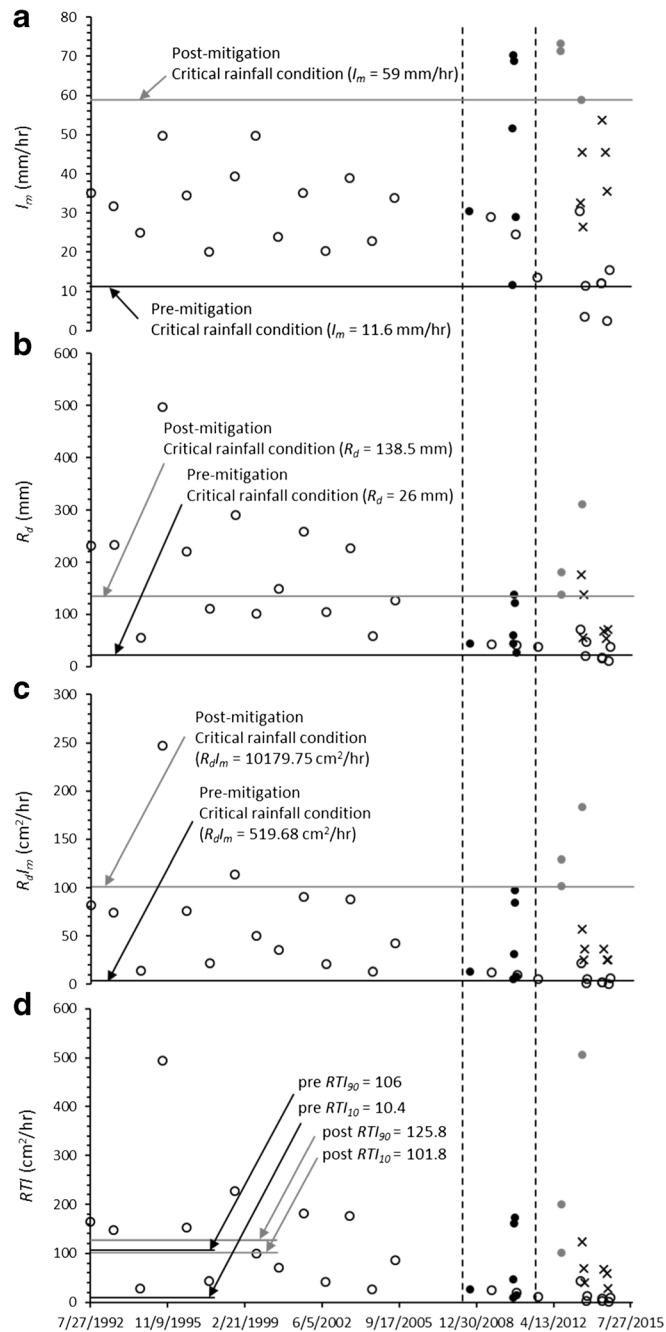


Fig. 10 The variations in the rainfall parameters contributing to the pre- and post-mitigation debris flows in the Wenjia Gully. Dash lines represent the Wenchuan Earthquake and completion of the mitigation system. The rainfall parameters have been significantly modified after implementing the mitigation system. RI considers both rainfall intensity and cumulative rainfall. RTI_{90} represents the upper critical line which is defined as upper 90% for the rainfall events. RTI_{10} is the lower critical line which is defined as the lowest value associated with a debris flow

2004; Huang et al. 2015a). The RTI_{90} and RTI_{10} represent the upper and lower critical lines for the events, respectively.

The variations in the number and volume of the debris flows as well as the associated rainfall thresholds are of direct interest in evaluating the performance of the mitigation system. As shown in Fig. 10, since no known debris flows existed before the earthquake, the increased number of debris flows are prominent, but it decreased abruptly with sharp increases in the critical rainfall parameters after implementing the mitigation system.

Notwithstanding the complex and dynamic interplays between rainfall and debris flow, plotting the occurrences in such fashion offers an intuitive representation on the variations in the number of debris flow events and rainfall thresholds. A single critical rainfall parameter (I_m or R_d) shows tendency to overestimate debris flow occurrences for the pre-/post-mitigation cases (Fig. 10a, b), and therefore, RI and RTI are employed to better characterize the critical conditions and the variations after implementing the mitigation system (Fig. 10c, d).

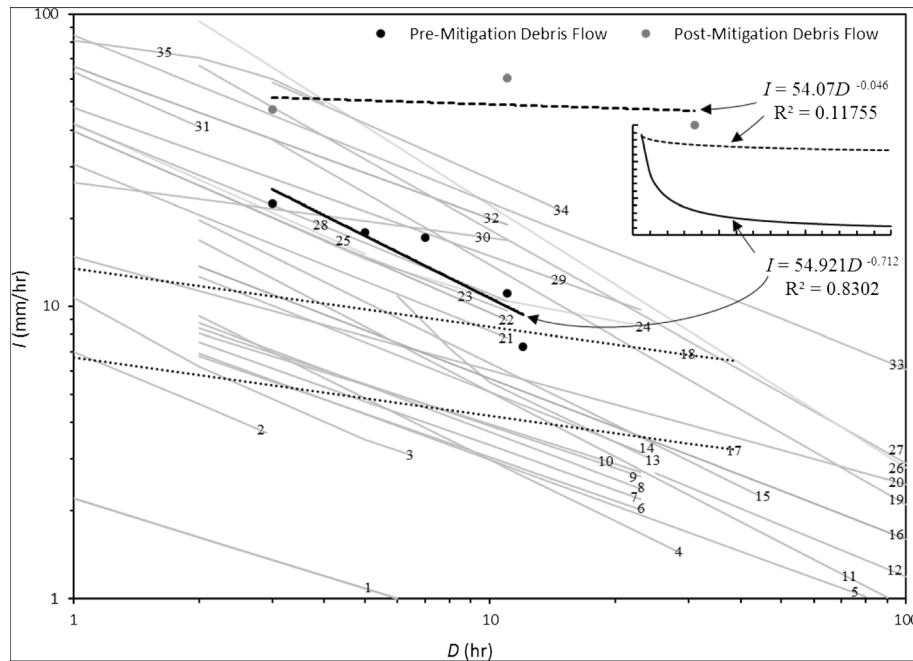


Fig. 11 Mean rainfall I - D thresholds for pre-/post-mitigation debris flows in the Wenjia Gully and other global and regional thresholds proposed in the previous research (references see Table 2). The poor correlation in the post-mitigation I - D threshold can be attributed to the limited data. A sharp escalation in the I - D threshold can be observed after implementing the mitigation system

The mean rainfall intensity-duration (I - D) thresholds are used to further evaluate the performance of the system. The pre-mitigation I - D thresholds were established from the five debris flows occurred before implementation of the system ($I = 54.921D^{-0.712}$), and the three events occurring afterwards were used to establish the post-mitigation I - D thresholds ($I = 54.07D^{-0.046}$).

The mean rainfall intensity decreases linearly as rainfall duration increases on a log-scale before the mitigation system; however, it remains almost unchanged with an increasing duration in the post-mitigation scenario (Fig. 11). The pre-mitigation I - D threshold for the Wenjia Gully is higher than many of the proposed global and regional thresholds, but the post-mitigation I - D threshold is considerably higher than any of the proposed values in Table 2, indicating a drastic change in the I - D curves due to the mitigation system. Decreases in the regional I - D thresholds are typical after a strong earthquake, but changes in the pre-/post-mitigation thresholds of a debris flow site are rarely assessed. In the pre-/post-mitigation rainfall I - D curves on a linear scale (Fig. 11), rainfall duration shows little correlation with debris flow occurrences after implementation of the system, which implies that loose deposits are more prone to debris flow under intense surface run-off but less affected by the pore water conditions.

The empirical relations between I_{max} , R_{cb} and debris flow volume, V , are presented in Fig. 12. Strong correlations are found between I_{max} and post-mitigation V as well as R_{cb} and post-mitigation V , which are noticeably higher than that of the pre-mitigation cases. As presented in Fig. 12, the ratios between R and pre-mitigation V can be used for a simplified extreme value analysis which estimates a maximum and minimum V for an observed R_{cb} assuming the absence of the mitigation system, and such estimations are substantially higher than the observed values. For the case of the debris flow that occurred on July 8, 2013, the estimated volume ranges 8×10^6 – 1×10^6 m³ (27 to 3 times greater than that

observed). Assuming the same geologic and topographic environments existed, the consequences would have been catastrophic.

The total depletion of the loose deposits in the gully is estimated as 5×10^6 m³ (about 10% of the overall deposit) after nine large-scale debris flows, assuming no new supplies in the sediment flux. Although the amount of the source material decreases and localized morphological conditions change after each debris flow, a large volume of loose deposit still exists in the gully which would be transformed into source material for subsequent debris flows, so it is logical to anticipate a continuous severe impact to the local community without the new mitigation system.

Concluding remarks

A predicament for the mitigation system in the Wenjia Gully is that a large amount of loose material (est. 50×10^6 m³) has been deposited in the gully by the co-seismic landslide. With a catchment area of 4 km² (greater than 50% of the catchment of the study area), debris flows in the gully are almost inevitable under saturation, and thus the core of the mitigation system is not only to prevent loose deposits from being mobilized and transformed into debris flows but also to reduce the frequency and magnitude of events.

This paper summarizes the co-seismic landslide and the subsequent debris flows in the Wenjia Gully after the Wenchuan Earthquake as well as the implementation of a novel debris flow mitigation system. It discusses the characteristics and relations between rainfall and debris flows to evaluate the performance of the system. The design of the mitigation system re-prioritized the focus from escalating the number and size of barriers and dams for sediment control to minimizing the saturation and agitation of the loose deposits in the gully; it describes the implementation of (1) a water-sediment segregation system to re-route the water from the debris flow through a drainage tunnel (water

Table 2 Some global and regional mean rainfall intensity-duration (*I-D*) thresholds for debris flows

No.	Area	Equation	Reference
1	Global	$I = 2.2D^{-0.44}$	(Guzzetti et al. (2008))
2		$I = 7.0D^{-6.00}$	(Cannon and Gartner (2005))
3	USA	$I = 1.7 + 9D^{-1.00}$	(Wieczorek (1987))
4	Italy	$I = 15D^{-7.00a}$	(Marchi et al. (2002))
5	USA	$I = 9.9D^{-0.52a}$	(Montgomery et al. (2000))
6	Italy	$I = 9.521D^{-0.4955}$	(Bolley and Oliaro (1999); Calcaterra et al. (2000); Guzzetti et al. (2007))
7		$I = 10.67D^{-0.5043}$	
8		$I = 12.649D^{-0.5324}$	
9		$I = 11.698D^{-0.4783}$	
10		$I = 11.0D^{-0.4459}$	
11		$I = 28.1D^{-0.74a}$	
12	Japan	$I = 1.35 + 55D^{-1.0a}$	(Hong et al. (2005))
13	USA	$I = 2.5 + 300D^{-2.0}$	(Cannon and Ellen (1985))
14	Italy	$I = 18.675D^{-0.565}$	(Ceriani et al. (1992); Zimmermann (1997); Guzzetti et al. (2007))
15	Switzerland	$I = 32D^{-0.70a}$	
16	Italy	$I = 20.1D^{-0.55a}$	
17	Taiwan	$I = 6.7D^{-0.2b}$	(Jan and Chen (2005); Chen (2011))
18		$I = 13.5D^{-0.2c}$	
19	Puerto Rico	$I = 91.46D^{-0.82}$	(Larsen and Simon (1993))
20	Global	$I = 14.82D^{-0.39}$	(Caine (1980))
21		$I = 30.53D^{-0.57}$	(Jibson (1989))
22	Japan	$I = 39.71D^{-0.62}$	
23	USA	$I = 35.23D^{-0.54}$	
24		$I = 6.9 + 30D^{-1.0}$	
25	China	$I = 49.11 - 6.81D^{1.0}$	
26	Italy	$I = 176.4D^{-0.90}$	
27	Taiwan	$I = 115.47D^{-0.8}$	(Chen et al. (2005))
28	Hong Kong	$I = 41.83D^{-0.58}$	(Jibson (1989))
29	Italy	$I = 47.742D^{-0.507}$	(Paronuzzi et al. (1998))
30	USA	$I = 26.51D^{-0.19}$	(Jibson (1989))
31	Brazil	$I = 63.38 - 22.19D^{1.0}$	
32	Puerto Rico	$I = 66.18D^{-0.52}$	
33	Portugal	$I = 84.3D^{-0.57a}$	(Jan and Chen (2005))
34	USA	$I = 116.48D^{-0.63}$	(Wieczorek et al. (2000))
35	Indonesia	$I = 92.06 - 10.68D^{1.0}$	(Jibson (1989))

I mean rainfall intensity (mm/h), *D* rainfall duration (h)

^a Applicable to all types of landslide

^b *I-D* thresholds after the Chi-Chi Earthquake

^c *I-D* thresholds before the Chi-Chi Earthquake

control), (2) active measures to stabilize the sediments in the midstream and downstream section of the gully (sediment control), and (3) a stepped flexible drainage channel connecting the upstream and outlet of the gully to prevent channelized erosion (erosion control). The

mitigation system has exhibited excellent performance and resilience to debris flows in the Wenjia Gully since implementation. The critical rainfall thresholds were substantially increased and susceptibility to debris flow is reduced.

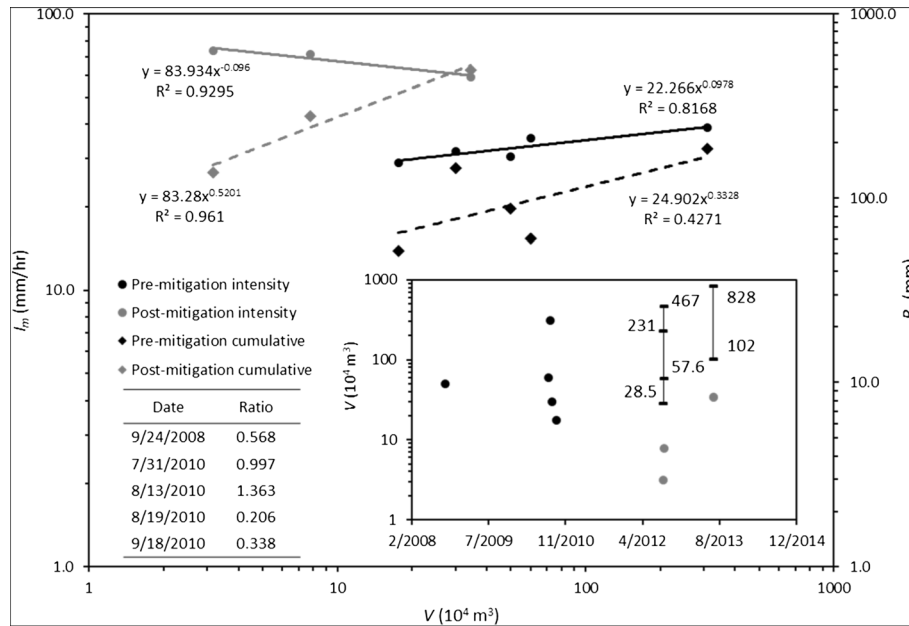


Fig. 12 Empirical correlations between I_m , R_d and V before and after implementing the mitigation system. Strong correlations are shown for the post-mitigation cases, with significant changes in the pre-/post-mitigation correlations, which indicate modifications on the characteristics of the rainfall-induced debris flows due to the mitigation system. Ratios between R_d and pre-mitigation V are used to estimate the V_{max} and V_{min} of the potential debris flows, assuming no mitigation system. Comparison of V and the estimations shows substantial differences

The novel mitigation system in the Wenjia Gully is not a universal solution that can be replicated and applied to other gullies. The uniqueness of each gully must be carefully considered in the design as the geological environment varies in each case. Each debris flow needs to be viewed as an individual event to understand the evolution of the failure process. The catastrophic damage caused by the debris flows between 2008 and 2011 is the result of failing to understand the characteristics of the gully; it severely underestimated the volume of the loose deposit after a strong earthquake. The design of any effective debris flow mitigation system, regardless of the size and cost, must start with a deep understanding of the area as well as the creativity of utilizing the nature of the study area as the basis of the design.

Acknowledgements

This work was financially supported by the Fund for Creative Research Groups of China (Grant No.41521002), Specialized Research Fund for the Doctoral Program of Higher Education of China (Grant No.20135122130002), and the Open Research Fund from the State Key Laboratory of Geohazard Prevention and Geoenvironmental Protection (Grant No. SKLGP2015K001). Authors are grateful to the field work and data collection by L. Chen and G.L. Yin.

References

Bolley S, Oliaro P (1999) Analisi dei debris flows in alcuni bacini campione dell'Alta Val Susa. *Geing Ambient e Mineraria*, Marzo:69–74
 Caine N (1980) The rainfall intensity: duration control of shallow landslides and debris flows. *Phys Geogr* 62:23–27

Calcaterra D, Parise M, Palma B, Pelella L (2000) The influence of meteoric events in triggering shallow landslides in pyroclastic deposits of Campania, Italy. In: *landslides in research, theory and practice*. In: Proceedings of the 8th international symposium on landslides held in Cardiff on 26–30 June 2000. Thomas Telford Publishing, London, pp 1–209
 Cannon SH, Ellen SD (1985) Rainfall conditions for abundant debris avalanches, San Francisco Bay region, California. *Calif Geol* 38:267–272
 Cannon SH, Gartner JE (2005) Wildfire-related debris flow from a hazards perspective. In: *Debris-flow hazards and related phenomena*. Springer, New York City, pp 363–385
 Cannon SH, Gartner JE, Wilson RC et al (2008) Storm rainfall conditions for floods and debris flows from recently burned areas in southwestern Colorado and southern California. *Geomorphology* 96:250–269
 Ceriani M, Lauzi S, Padovan N (1992) Rainfalls and landslides in the alpine area of Lombardia region, central Alps, Italy. In: *Proc. Int. Symp. Interpraevent*. pp 9–20
 Chen C-Y, Chen T-C, Yu F-C et al (2005) Rainfall duration and debris-flow initiated studies for real-time monitoring. *Environ Geol* 47:715–724. doi:10.1007/s00254-004-1203-0
 Chen JC (2011) Variability of impact of earthquake on debris-flow triggering conditions: case study of Chen-Yu-Lan watershed, Taiwan. *Environ Earth Sci* 64:1787–1794. doi:10.1007/s12665-011-0981-4
 Chen JC, Jan CD, Huang WS (2013) Characteristics of rainfall triggering of debris flows in the Chenyulan watershed, Taiwan. *Nat Hazards Earth Syst Sci* 13:1015–1023. doi:10.5194/nhess-13-1015-2013
 Costa JE, Wieczorek GF (1987) Debris flows/avalanches: process, recognition, and mitigation. Geological Society of America
 deWolfe VG, Santi PM, Ey J, Gartner JE (2008) Effective mitigation of debris flows at Lemon Dam, La Plata County, Colorado. *Geomorphology* 96:366–377. doi:10.1016/j.geomorph.2007.04.008
 Glade T, Crozier M, Smith P (2000) Applying probability determination to refine landslide-triggering rainfall thresholds using an empirical “antecedent daily rainfall model.”. *Pure Appl Geophys* 157:1059–1079
 Guzzetti F, Peruccacci S, Rossi M, Stark CP (2007) Rainfall thresholds for the initiation of landslides in central and southern Europe. *Meteorog Atmos Phys* 98:239–267
 Guzzetti F, Peruccacci S, Rossi M, Stark CP (2008) The rainfall intensity–duration control of shallow landslides and debris flows: an update. *Landslides* 5:3–17
 Hong Y, Hiura H, Shino K et al (2005) The influence of intense rainfall on the activity of large-scale crystalline schist landslides in Shikoku Island, Japan. *Landslides* 2:97–105
 Huang J, Huang RQ, Ju NP et al (2015a) 3D WebGIS-based platform for debris flow early warning: a case study. *Eng Geol* 197:57–66

- Huang J, Ju NP, Liao YJ, Liu DD (2015b) Determination of rainfall thresholds for shallow landslides by a probabilistic and empirical method. *Nat Hazards Earth Syst Sci* 15:2715–2723
- Huang R, Fan X (2013) The landslide story. *Nat Geosci* 6:325–326. doi:10.1038/ngeo1806
- Iverson RM (1997) The physics of debris flows. *Rev Geophys* 35:245–296
- Jan C-D, Chen C-L (2005) Debris flows caused by typhoon herb in Taiwan. In: *Debris-flow hazards and related phenomena*. Springer, New York City, pp 539–563
- Jan C, Lee M, Huang T (2002) Rainfall threshold criterion for debris-flow initiation. *Natl Cheng K Univ:9104–9112 (in Chinese)*
- Jan CD, Lee MH (2004) A debris-flow rainfall-based warning model. *J Chin Soil Water Conserv* 35:275–285
- Jibson RW (1989) Debris flows in southern Puerto Rico. *Geol Soc Am Spec Pap* 236:29–56
- Larsen MC, Simon A (1993) A rainfall intensity-duration threshold for landslides in a humid-tropical environment. *Puerto Rico Geogr Ann Ser A Phys Geogr*:13–23
- Marchi L, Arattano M, Deganutti AM (2002) Ten years of debris-flow monitoring in the Moscardo Torrent (Italian Alps). *Geomorphology* 46:1–17
- Ministry of Land and Resources of China (2006) Specification of Geological Investigation for Debris Flow Stabilization (DZ/T0020).
- Montgomery DR, Schmidt KM, Greenberg HM, Dietrich WE (2000) Forest clearing and regional landsliding. *Geology* 28:311–314
- Ni HY, Zheng WM, Tie YB et al (2012) Formation and characteristics of post-earthquake debris flow: a case study from Wenjia gully in Mianzhu, Sichuan, SW China. *Nat Hazards* 61:317–335
- Paronuzzi P, Cocolo A, Garlatti G (1998) Eventi meteorici critici e debris flows nei bacini montani del Friuli. *L'Acqua, Sez I/Memorie* 6:39–50
- Tang C, Van Asch TWJ, Chang M et al (2012) Catastrophic debris flows on 13 August 2010 in the Qingping area, southwestern China: the combined effects of a strong earthquake and subsequent rainstorms. *Geomorphology* 139–140:559–576. doi:10.1016/j.geomorph.2011.12.021
- Wang Y, Yin M, Tang L et al (2014) Investigation of vegetation in Wenjiagou Debris Flow Area. *J Agric For* 4:63–67 (in Chinese)
- Wieczorek GF (1987) Effect of rainfall intensity and duration on debris flows in central Santa Cruz Mountains. In: *Debris flow/avalanches: process, recognition, and mitigation*. Geological Society of America, Reviews in Engineering Geology 7. pp 93–104
- Wieczorek GF, Morgan BA, Campbell RH (2000) Debris-flow hazards in the Blue Ridge of central Virginia. *Environ Eng Geosci* 6:3–23
- Xu Q (2010) The 13 August 2010 catastrophic debris flows in Sichuan Province: characteristics, genetic mechanism and suggestions. *J Eng Geol* 18:596–608 (in Chinese)
- Xu Q, Pei X, Huang R (2009) Large-scale landslides induced by the Wenchuan Earthquake. Science Press, Beijing (in Chinese)
- Xu Q, Zhang S, Li WL, Van Asch TWJ (2012) The 13 August 2010 catastrophic debris flows after the 2008 Wenchuan earthquake, China. *Nat Hazards Earth Syst Sci* 12:201–216. doi:10.5194/nhess-12-201-2012
- Yu B, Ma Y, Wu Y (2013) Case study of a giant debris flow in the Wenjia Gully, Sichuan Province, China. *Nat Hazards* 65:835–849. doi:10.1007/s11069-012-0395-y
- Yu B, Zhu Y, Wang T et al (2014) A prediction model for debris flows triggered by a runoff-induced mechanism. *Nat Hazards* 74:1141–1161. doi:10.1007/s11069-014-1234-0
- Zhou GGD, Cui P, Tang JB et al (2014) Experimental study on the triggering mechanisms and kinematic properties of large debris flows in Wenjia Gully. *Eng Geol*. doi:10.1016/j.enggeo.2014.10.021
- Zhuang J, Iqbal J, Peng J, Liu T (2014) Probability prediction model for landslide occurrences in Xi'an, Shaanxi Province, China. *J Mt Sci* 11:345–359
- Zimmermann M (1997) Murganggefahr und Klimaänderung-ein GIS-basierter Ansatz. vdf Hochschulverlag AG

F. Liu · Q. Xu (✉) · X. Dong · B. Yu · H. Li

State Key Laboratory of Geohazard Prevention and Geoenvironment Protection, Chengdu University of Technology, Chengdu, Sichuan, China
e-mail: xuqiang_68@126.com

F. Liu · J. Frost

School of Civil and Environmental Engineering, Georgia Institute of Technology, Atlanta, GA, USA